

# Surface properties and hemocompatibility of alkyl-siloxane monolayers supported on silicone rubber: effect of alkyl chain length and ionic functionality

James H. Silver<sup>a,1</sup>, Jui-Che Lin<sup>a,2</sup>, Florencia Lim<sup>a,3</sup>, Vassiliki A. Tegoulia<sup>b,\*</sup>,  
Manoj K. Chaudhury<sup>c</sup>, Stuart L. Cooper<sup>d</sup>

<sup>a</sup>Department of Chemical Engineering, University of Wisconsin, Madison, WI 53706, USA

<sup>b</sup>Department of Chemical Engineering, University of Delaware, Newark, DE 19716, USA

<sup>c</sup>Department of Chemical Engineering, Lehigh University, Bethlehem, PA 18015, USA

<sup>d</sup>Illinois Institute of Technology, Chicago, IL 60616, USA

Received 1 April 1998; accepted 22 July 1998

## Abstract

Self-assembled monolayers of alkylsiloxanes supported on poly(dimethylsiloxane) (PDMS) rubber were used as model systems to study the relation between blood compatibility and surface composition. The inner lumen of PDMS tubes were first treated with an oxygen plasma. The resultant oxidized surfaces were post-derivatized by reaction with alkyltrichlorosilanes to form the monolayer films. The alkyl chain lengths used were slightly longer than in a previous study, and this may alter the phase-state of the monolayer from liquid-like to crystalline. The chemical properties of the monolayer were controlled by varying the chemical composition of the alkyltrichlorosilanes used. Terminal functionalities included  $-\text{CH}_3$ ,  $-\text{CF}_3$ ,  $-\text{COOH}$ ,  $-\text{SO}_3\text{H}$  and  $-(\text{CH}_2\text{CH}_2\text{O})_4\text{OH}$ . Surface derivatization was verified with static contact angle measurements and X-ray photoelectron spectroscopy. Blood compatibility was evaluated using a canine ex vivo arterio-venous series shunt model. Surfaces grafted with hydrophobic head groups such as  $-\text{CH}_3$  and  $-\text{CF}_3$  were significantly less thrombogenic than the surfaces composed of ionic head groups such as  $-\text{COOH}$  and  $-\text{SO}_3\text{H}$ . Surfaces enriched in  $-(\text{CH}_2\text{CH}_2\text{O})_4\text{OH}$  had an intermediate thrombogenicity. Silastic pump grade tubing and polyethylene tubing, used as controls, were found to be the least thrombogenic of all the surfaces tested. © 1999 Elsevier Science Ltd. All rights reserved.

**Keywords:** Self-assembled monolayer; Surface modification; Blood compatibility; Silicone rubber

## 1. Introduction

One of the central ideas of biomaterials research is that there is a relationship between chemistry of an implanted device or material and its hemocompatibility. No study is considered complete without an evaluation of the surface properties of the biomaterial in question. For many of these materials, however, the surface chemistry is quite

complex, and it is difficult to be sure of the chemical composition at the blood–biomaterial interface. Many commercially available materials, such as Biomer<sup>®</sup>, may contain surface-active additives, such as antioxidants or processing aids, which further complicates interpretation of blood–material interactions [1]. Multiphase materials such as polyurethanes may show surface reorientation between the dry and hydrated states [2], making it difficult to evaluate the surface composition using methods in which the polymer surface is analyzed in air or in vacuo.

Recently, much interest has arisen in self-assembled monolayers (SAMs), with the goal of developing molecular-level control over surface properties, both for fundamental studies of adhesion and wettability, as well as for technological applications [3]. These films are typically formed by the adsorption of terminally functionalized alkanethiols ( $\text{HS}(\text{CH}_2)_n\text{X}$ ) onto gold substrates [4], or

\* Corresponding author.

<sup>1</sup> Current address: Orthogene Inc., 34700 Campus Drive, Fremont, CA 94555, USA.

<sup>2</sup> Current address: Department of Chemical Engineering, National Cheng Kung University, Tainan, Taiwan 70101, ROC.

<sup>3</sup> Current address: Guidant Corporation, 3200 Lakeside Drive, Santa Clara, CA 95054, USA.

the adsorption of terminally functionalized silanes onto silicon surfaces, glass, or fused silica [5]. Formation of SAMs on elastomeric materials such as poly(dimethylsiloxane) (PDMS) has recently been demonstrated as well [6–9]. The perfection of these monolayers was inferred from contact angle measurements while infrared dichroism was used to confirm ordering in the hydrocarbon chains. The thickness of SAMs on PDMS was estimated based on a comparison with monolayers formed on polished silicon wafers [8].

The interactions of these surfaces with biological molecules have been under investigation. A number of reports have appeared which suggest that cellular adhesion on self-assembled monolayers can be controlled by the chemistry of the underlying surface [5]. Others have used the control provided by SAMs to direct protein adsorption onto such surfaces [10]. However, the interactions between larger, more complex proteins such as fibronectin with SAMs are still difficult to control, and result in a number of different cellular responses [11, 12]. Little information is available regarding the blood compatibility of such surfaces.

In order to carefully control the structure of our blood-contacting surfaces, we have functionalized the surface of poly(dimethylsiloxane) in a two-step process, using specific chemistries to form surface monolayers with known compositions. In the first step, the surface is oxidized using an oxygen plasma, and in the second step, a monolayer is formed by chemisorption of alkyltrichlorosilanes ( $\text{Cl}_3\text{Si}(\text{CH}_2)_n\text{R}$ ) onto the surface of the polymer [6]. Previous work [6–9, 13] has shown that these methods create well-defined silane monolayers whose surface chemistry is controlled by the head group functionalities (R) of the silanes. The functionalities studied were methyl ( $-\text{CH}_3$ ), trifluoromethyl ( $-\text{CF}_3$ ), ethylene oxide ( $-(\text{OCH}_2\text{CH}_2)_4\text{OH}$ ), carboxylate ( $-\text{COOH}$ ), and sulfonate ( $-\text{SO}_3\text{H}$ ).

Previously, we have reported on the blood compatibility of a related series of self-assembled monolayers supported on silicone rubber [14]. In the present study, head groups with sulfonate and carboxylate functionalities are included. One of the primary differences between the two studies is the length of the alkyl tail in the subsurface region of the monolayer. Longer alkyl chains, used in the present study, have been shown, by infrared spectroscopy, to form a more extended, crystalline structure for self-assembled monolayers on PDMS. In contrast, the shorter alkyl chains, investigated in the previous study were found to be in a more mobile, liquid-like phase [14]. It has long been postulated that crystalline, less mobile surfaces do not enhance blood compatibility. By comparing the thrombogenicity of these new longer monolayers with results from the previous study we will try to test this hypothesis.

Another hypothesis we would like to test is that fluorination of a surface leads to a more biocompatible sur-

face. GoreTex<sup>®</sup> vascular grafts are made from expanded poly(tetrafluoroethylene) (e-PTFE), and a great deal of clinical experience has been obtained with this material. Incorporation of fluorine groups by radiation grafting has been previously attempted by Hoffman et al. [15], who found that when woven Dacron vascular grafts were modified with a tetrafluoroethylene plasma, the hemocompatibility of these materials was significantly improved [16]. Further, they found that although less fibrinogen was adsorbed on TFE-Dacron, it was less elutable by sodium dodecyl sulfate. However, after plasma modification, the surface showed a variety of functional groups, including  $\text{CF}_3$ ,  $\text{CF}_2$ ,  $\text{CF}-\text{CF}_n$ ,  $\text{CF}$ , and  $\text{C}-\text{CF}_n$ , as determined from the high resolution Cls peak in the ESCA spectrum so that the surface properties could be attributed to a specific functional group. In the present study, a surface exposing only  $\text{CF}_3$  functional groups with expected high interfacial free energy [17] is compared with more hydrophilic, lower interfacial free energy surfaces.

The poly(ethylene oxide) (PEO) terminated monolayer has been included to examine if incorporation of PEO results in surfaces with improved biocompatibility. Previous work has shown that surfaces incorporating long PEO chains were blood compatible [18, 19]. On the contrary, shorter PEO chains endlinked on poly(glycidoxypopyl methyl-dimethyl siloxane) via their terminal hydroxyl groups were found to enhance platelet and fibrinogen deposition in an ex vivo shunt [19]. This was attributed to an incomplete coverage of the surface by the PEO chains. However, protein adsorption and cell adhesion on thiol self-assembled monolayers containing only three or six ethylene oxide groups was found to be minimal in vitro [20, 21].

A number of investigators have shown that polymers incorporating sulfonate or carboxylate groups have rather remarkable blood-contacting properties. These materials may act like heparin, a mucopolysaccharide which is clinically used as an anticoagulant. Sulfate, amino-sulfate, and carboxylate groups have been shown to be essential to the anticoagulant activity of heparin [22]. Jozefovicz and Jozefowicz [23] have modified polystyrenes and dextrans to incorporate these ionic groups, and have shown that these materials possess anticoagulant, heparin-like, activity. However, it was found that sulfonate groups were essential for heparin-like activity, but carboxylate groups, while greatly enhancing such activity, were non-essential. Dextrans which contained only carboxylate groups were determined to be inactive [24]. Ito et al. [25] have shown that polyurethanes grafted with poly(vinyl sulfonate) possessed heparin-like activity, which was reduced upon incorporation of carboxylate groups, contrary to the results of Jozefovicz and Jozefowicz. Okkema et al. found that the incorporation of carboxylate groups did not improve the hemocompatibility of

polyurethanes, as evaluated in a canine ex vivo model [26].

In experiments with water soluble sulfonated polyurethanes, it was shown that these polymers prolong clotting times, inhibit the process of fibrin assembly, and inhibit thrombin activity [27]. Polyurethanes grafted with propyl sulfonate groups and containing PTMO as the macroglycol show strong antithrombotic behavior, with low levels of platelet deposition or spreading [26]. Similar results were also obtained when Biomer<sup>®</sup>, a commercial polyurethaneurea containing PTMO as the macroglycol, was sulfonated [28]. Polyurethanes surface grafted with poly(ethylene oxide) chains which are end-terminated with sulfonate groups significantly prolong occlusion times in a rabbit A–A shunt model [29]. Santerre et al. [30] have shown that sulfonated polyurethanes interact strongly with fibrinogen, and that fibrinogen is not displaced from these surfaces in Vroman-effect-type experiments. Thus, polymers containing sulfate or sulfonate groups have very interesting behavior in contact with blood.

The hemocompatibility of the silicone elastomer and surface-derivatized silicone elastomers was evaluated using a canine ex vivo series shunt model [31]. PE tubing was also used as a control surface. The monolayer formation and surface composition of these elastomers after modification was examined using X-ray photoelectron spectroscopy. Surface energetics were evaluated by contact angle measurements. Throughout the paper, the term ‘thromboresistant’ is used to refer to materials which show low platelet or thrombus deposition on their surfaces.

## 2. Materials and methods

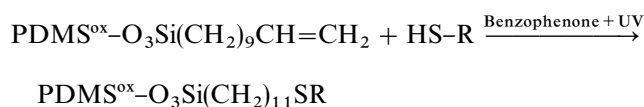
### 2.1. Materials

Silicone rubber tubing (0.125" ID) (RX Pump Grade, Lot No. HH031678) and five surface-modified Silastic tubings were received from Dow Corning, and stored in distilled water until use. The surfaces were modified to contain  $-\text{CH}_3$ ,  $-\text{CF}_3$ ,  $-(\text{CH}_2\text{CH}_2\text{O})_4\text{OH}$ ,  $-\text{COOH}$ , or  $-\text{SO}_3\text{H}$  functional groups. Polyethylene tubing (0.125" ID) was purchased from Clay-Adams (Intramedic, Parsippany, NJ, Lot #93485).

### 2.2. Surface modification of PDMS

Nine segments of PDMS (Silastic) tubing each about 5.5" long (0.118" ID; 0.25" OD), were oxidized in a Harlick plasma cleaner for 5 min in an oxygen atmosphere (0.4 Torr). The oxidized segments were joined together with short polyethylene tubes, and subsequently filled with a silanizing solution. The silanizing solution was prepared by dissolving alkyltrichlorosilanes in per-

fluorooctane at concentrations of 10–20  $\mu\text{g silane g}^{-1}$  of solvent. After 1 h, the tubes were rinsed with fresh perfluorooctane, followed by ethanol and then dried under a continuous stream of air. The silanes used for these studies were:  $\text{Cl}_3\text{Si}(\text{CH}_2)_{15}\text{CH}_3$  (Petrach);  $\text{Cl}_3\text{Si}(\text{CH}_2)_2\text{CF}(\text{CF}_3)\text{CF}_2\text{CF}(\text{CF}_3)_2$  (Dow Corning, Courtesy of Dr G. Gornowitz) and  $\text{Cl}_3\text{Si}(\text{CH}_2)_9\text{CH}_2=\text{CH}_2$  (Dow Corning). The fluorosilane contained about 15% of the following isomer:  $\text{Cl}_3\text{Si}(\text{CH})\text{CH}_3\text{CF}(\text{CF}_3)\text{CF}_2\text{CF}(\text{CF}_3)_2$ . The purity of the other two silanes was better than 99%. The olefin-terminated PDMS were further reacted with  $\text{HS}(\text{CH}_2)_2\text{SO}_3\text{Na}$  and  $\text{HS}(\text{CH}_2)_2(\text{OCH}_2\text{CH}_2)_4\text{OH}$  by a free radical process in order to introduce the ethylene oxide and sulfonate groups on its surface as shown:



where  $\text{R} = -(\text{CH}_2)_2\text{SO}_3\text{Na}$  and  $-(\text{CH}_2)_2(\text{OCH}_2\text{CH}_2)_4\text{OH}$ . In separate experiments, carboxylic acid groups were introduced on the surface of  $\text{PDMS}^{\text{ox}}-\text{O}_3\text{Si}(\text{CH}_2)_9\text{CH}=\text{CH}_2$ , by oxidizing the olefin groups of the monolayers by a mixture of potassium permanganate and potassium periodate according to the procedure of Wasserman and Whitesides [32].

### 2.3. Surface property characterization

X-ray photoelectron spectroscopy (XPS) spectra were obtained using a Perkin–Elmer Physical Electronics, PHI 5400 spectrometer. Samples of each tube were cut in half lengthwise, and flattened in order to hold them onto the sample stage. A magnesium anode operating at 300 W and 15 kV and photoelectron take-off angle of 45° was used. The take-off angle is defined as the angle between the detector and the normal of the substrate. Survey spectra (0–1000 eV) were taken at a pass energy of 90 eV using a 1000  $\mu\text{m}$  diameter X-ray spot size. The relative atomic percentage of each element at the surface was estimated from the peak areas using atomic sensitivity factors specified for the PHI 5400. High-resolution spectra of the O1s peak, the N1s peak, the C1s, peak, the Si2p peak, and the F1s peak at a pass energy of 17.9 eV were also taken.

Water-in-air static contact angles were measured on the concave inner lumen of these surfaces using the procedure of Lelah et al. [33]. Briefly, short tubes of PDMS were cut into hemicylindrical form. Small drops (ca. 1 mm) of water were placed on the inner lumen of these tubes, and were either photographed or analyzed by a video microscopy system. Tangent lines were drawn at the intersection of the drop and the PDMS surface by geometric construction directly on the photograph or on a replica of the video image to estimate the contact angles.

#### 2.4. Blood-contacting properties

The blood-contacting properties of these materials were evaluated using a canine *ex vivo* series shunt experiment with modifications [31]. The polymer tubings were cut into 1.5" length and assembled into shunts. Each polymer was present in triplicate in each shunt.

Adult mongrel dogs which were selected after hematological screening were injected with autologous  $^{111}\text{In}$ -labeled platelets and  $^{125}\text{I}$ -labeled fibrinogen. No anticoagulant was used in this procedure. The shunts were filled with sterile, degassed, divalent cation-free Tyrodes solution ( $0.2 \text{ g l}^{-1}$  KCl,  $8.0 \text{ g l}^{-1}$  NaCl,  $0.05 \text{ g l}^{-1}$   $\text{NaH}_2\text{PO}_4\text{-H}_2\text{O}$ ,  $1.0 \text{ g l}^{-1}$  dextrose,  $1.0 \text{ g l}^{-1}$   $\text{NaHCO}_3$ ,  $\text{pH} = 7.35$ ), and hydrated overnight at  $4^\circ\text{C}$ . The femoral artery and vein were cannulated with the shunt. A branch artery proximal to the shunt cannulation site was connected to a flushing system. The blood flow rate was continuously monitored during blood exposure using an electromagnetic flow probe. The initial flow rate was controlled at  $280 \pm 20 \text{ ml min}^{-1}$ . Blood samples were collected over time to determine bulk radioactivity, platelet and fibrinogen concentrations, hematocrit, blood gas and hematological function.

Three separate surgeries were performed. Shunts were run for 1, 2, 5, 10, 15, 20, 25, 30, 45, and 60 min of blood contact. At the end of each blood-contact interval, the femoral artery was clamped, and the bulk blood was flushed out of the shunt at a flow rate of approximately  $60 \text{ ml min}^{-1}$ , which gives a much lower shear rate than that during blood contact. Immediately following flushing, the test sections were removed, and the tubing contents were fixed with 2% glutaraldehyde. Then, test sections were subdivided into sections for gamma scintillation counting and for evaluation by scanning electron microscopy (SEM). Samples were prepared for scanning electron microscopy using the procedure previously described [34]. These samples were examined using a JEOL JSM-35C SEM at 15 kV accelerating voltage.

Platelet and fibrinogen deposition profiles were determined by counting the segments in a gamma counter (Gamma 5500, Beckman) and converting the number of counts into the number of platelets or mass of fibrinogen.

The average and standard deviations of the nine data points (three data points for each of three surgeries) were obtained. Outlier data points among the nine points were rejected at the 99% confidence level, using Nalimov's test [35]. Negative values (primarily fibrinogen data at short times) were set to zero.

### 3. Results and discussion

#### 3.1. Surface characterization

The presence of each surface functionality was verified using X-ray photoelectron spectroscopy (Table 1). For  $\text{PDMS}^{\text{ox}}\text{-O}_3\text{Si}(\text{CH}_2)_2\text{CF}(\text{CF}_3)\text{CF}_2\text{CF}(\text{CF}_3)_2$  a fluorine peak on the survey spectra provides a marker for the surface derivatization. Similarly, for the  $\text{PDMS}^{\text{ox}}\text{-O}_3\text{Si}(\text{CH}_2)_{11}\text{S}(\text{CH}_2)_2\text{SO}_3\text{H}$ , the surface concentration in sulfur is enhanced. Incorporation of the functional groups can also be accounted by the increased oxygen content for the oxygen containing functionalities. For all surfaces but the Silastic and  $\text{PDMS}^{\text{ox}}\text{-O}_3\text{Si}(\text{CH}_2)_{15}\text{CH}_3$ , the high resolution C1s spectra showed more than one peak to account for the presence of C–F, C–O and C=O bonds on the surface (data not shown). The majority of the materials show less C1s and more O1s than the Silastic pump grade tubing at a take-off angle of  $45^\circ$ . This increased oxygen content and decreased carbon content may be due to some loss of the monolayer as the tubes were flattened for XPS analysis and may have exposed some of the underlying PDMS material. No measurement of the surface thickness on these PDMS elastomers has been made. It is also not known how homogeneous these surfaces are, nor was information obtained about the size and nature of any defects. Circular dichroism and detailed XPS results obtained by Chaudhury and co-workers [7, 13] verified the model structure of monolayer surfaces on PDMS. However, such studies were not performed on our samples.

Static contact angle data obtained on these surfaces are shown in Table 2. Both  $\text{PDMS}^{\text{ox}}\text{-O}_3\text{Si}(\text{CH}_2)_{15}\text{CH}_3$  and  $\text{PDMS}^{\text{ox}}\text{-O}_3\text{Si}(\text{CH}_2)_2\text{CF}(\text{CF}_3)\text{CF}_2\text{CF}(\text{CF}_3)_2$  showed contact angles higher than  $100^\circ$  with the perfluoro-

Table 1  
XPS surface analysis<sup>a</sup>

Material	C1s	O1s	Si2p	S2p	F1s
$\text{PDMS}^{\text{ox}}\text{-O}_3\text{Si}(\text{CH}_2)_{10}\text{COOH}$	46.7	29.8	23.1	0.4	—
$\text{PDMS}^{\text{ox}}\text{-O}_3\text{Si}(\text{CH}_2)_{11}\text{S}(\text{CH}_2)_2\text{SO}_3\text{H}$	38.0	48.7	11.4	1.1	—
$\text{PDMS}^{\text{ox}}\text{-O}_3\text{Si}(\text{CH}_2)_{11}\text{S}(\text{CH}_2)_2(\text{OCH}_2\text{CH}_2)_4\text{OH}$	42.6	42.6	14.2	0.7	—
$\text{PDMS}^{\text{ox}}\text{-O}_3\text{Si}(\text{CH}_2)_2\text{CF}(\text{CF}_3)\text{CF}_2\text{CF}(\text{CF}_3)_2$	38.2	44.9	12.1	1.0	3.8
$\text{PDMS}^{\text{ox}}\text{-O}_3\text{Si}(\text{CH}_2)_{15}\text{CH}_3$	40.9	42.5	15.4	0.7	—
Silastic pump grade tubing	44.3	36.2	18.9	0.7	—

<sup>a</sup> The standard error is on the order of 10% or less according to information provided for the PHI spectrometer by the manufacturers.

methyl functionalized PDMS exhibiting the higher contact angle as expected. The remaining surfaces are found to be much less hydrophobic, the order of hydrophilicity being  $\text{PDMS}^{\text{ox}}-\text{O}_3\text{Si}(\text{CH}_2)_{11}\text{S}(\text{CH}_2)_2\text{SO}_3\text{H} < \text{PDMS}^{\text{ox}}-\text{O}_3\text{Si}(\text{CH}_2)_{11}\text{S}(\text{CH}_2)_2(\text{OCH}_2\text{CH}_2)_4\text{OH} < \text{PDMS}^{\text{ox}}-\text{O}_3\text{Si}(\text{CH}_2)_{10}\text{COOH}$ . However, the differences in hydrophilicity in the latter group are much less than that between this group and surfaces containing the methyl and perfluoromethyl terminal units. Based on the contact angle results as well as XPS data, we can say that the adsorbed films of alkylsiloxanes expose their terminal functionalities in such a way as to affect the chemistry and wettability of the surface. We acknowledge the fact that the surface density and close packing of the monolayers was not verified in this study. However, since a considerable amount of characterization has been done by Chaudhury and co-workers [6, 7] and the technique has been established as a successful one, we feel comfortable that the

surfaces are adequately modified so that their biocompatibility is strongly influenced by the terminal functionalities of the silane monolayers.

### 3.2. Blood-contacting properties

A material is considered to be thrombogenic if relatively large numbers of platelets and fibrinogen/fibrin molecules adhere to it during blood contact. A surface coverage of approximately 70–100 platelets per  $1000 \mu\text{m}^2$  represents a monolayer of platelets on the surface, although the degree of platelet spreading and activation can cause this number to vary [36].

Fig. 1 shows the transient platelet deposition profiles for the materials tested during the first hour of blood exposure. The platelet deposition profiles show a peak between 20 and 30 min of blood contact. The same trend has been previously reported for different polymeric materials in similar canine series shunt experiments. This peak reflects thrombus growth in competition with thrombus detachment (embolization). The RX Pump Grade tubing and PE had the lowest levels of platelet deposition. The  $-(\text{CH}_2\text{CH}_2\text{O})_4\text{H}$ ,  $-\text{CF}_3$ , and  $-\text{CH}_3$  surfaces all had intermediate levels of platelet deposition, with the first one having the highest levels of platelet deposition at early time points ( $<15$  min). Samples derivatized with  $-\text{COOH}$  and  $-\text{SO}_3\text{H}$  both had the highest levels of platelet deposition, with peak values of over 6000 platelets per  $1000 \mu\text{m}^2$  after 20 min of blood exposure.

The fibrinogen/fibrin deposition profiles for these materials are shown in Fig. 2. Silastic segments derivatized

Table 2  
Water-in-air contact angles on  $\text{PDMS}^{\text{ox}}-\text{O}_3\text{Si}(\text{CH}_2)_n\text{X}$

Material	Contact angle ( $\theta_{\text{H}_2\text{O}}$ )
$\text{PDMS}^{\text{ox}}-\text{O}_3\text{Si}(\text{CH}_2)_{10}\text{COOH}$	$59 \pm 4$
$\text{PDMS}^{\text{ox}}-\text{O}_3\text{Si}(\text{CH}_2)_{11}\text{S}(\text{CH}_2)_2\text{SO}_3\text{H}$	$50 \pm 2$
$\text{PDMS}^{\text{ox}}-\text{O}_3\text{Si}(\text{CH}_2)_{11}\text{S}(\text{CH}_2)_2(\text{OCH}_2\text{CH}_2)_4\text{OH}$	$54 \pm 3$
$\text{PDMS}^{\text{ox}}-\text{O}_3\text{Si}(\text{CH}_2)_2\text{CF}(\text{CF}_3)\text{CF}_2\text{CF}(\text{CF}_3)_2$	$109 \pm 4$
$\text{PDMS}^{\text{ox}}-\text{O}_3\text{Si}(\text{CH}_2)_{15}\text{CH}_3$	$104 \pm 1$
Silastic pump grade tubing	$108 \pm 1$

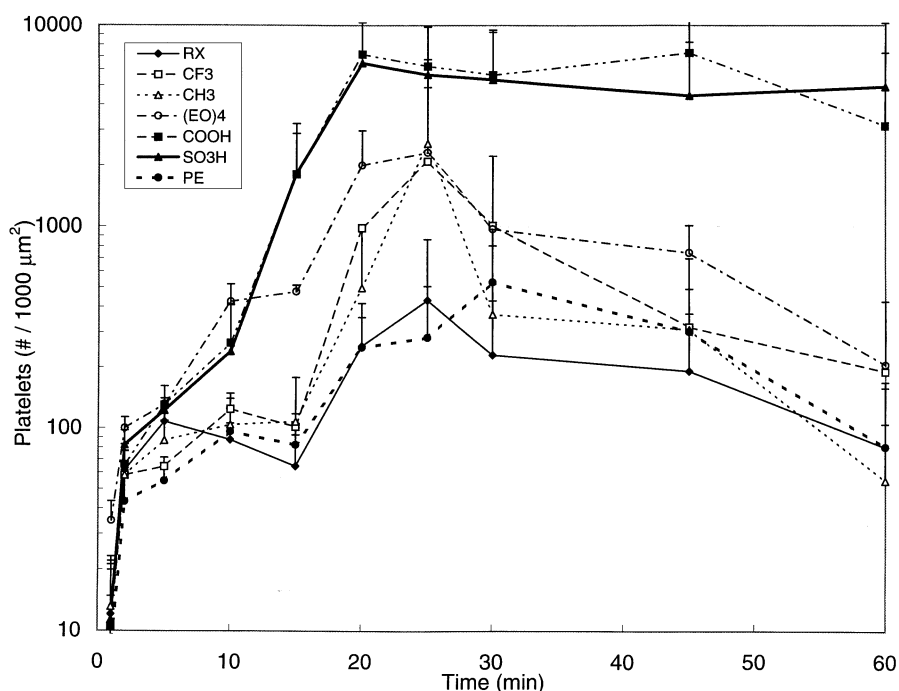


Fig. 1. Platelet deposition profiles during the initial hour of blood contact.

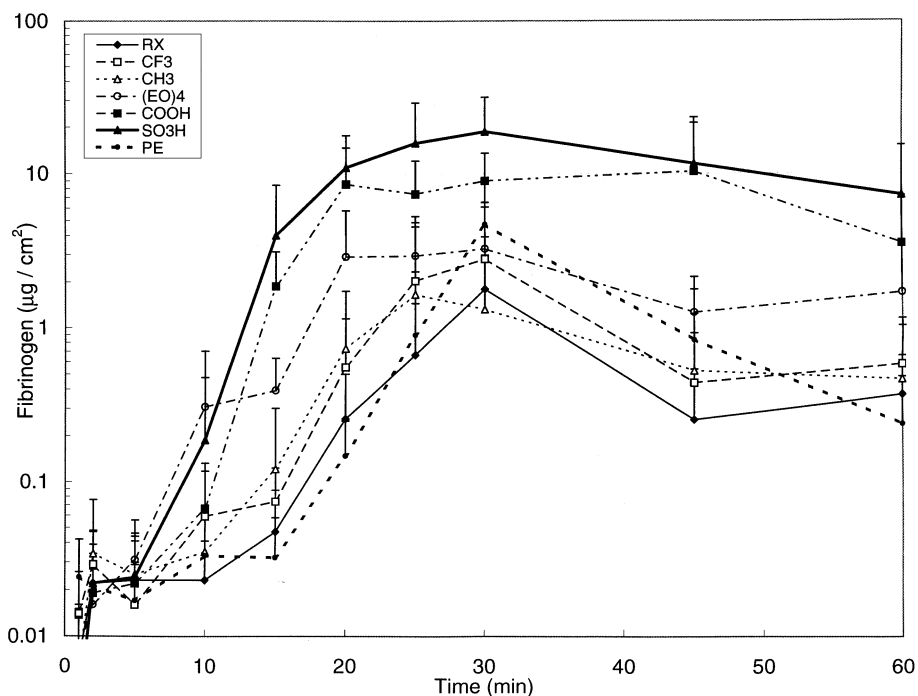


Fig. 2. Fibrinogen/fibrin deposition profiles during the initial hour of blood contact.

Table 3  
Platelet and fibrinogen deposition statistics relative rank

Material	Platelet rank	Fibrinogen rank
PDMS <sup>ox</sup> -O <sub>3</sub> Si(CH <sub>2</sub> ) <sub>10</sub> COOH	6.0 ± 1.2	4.9 ± 1.6
PDMS <sup>ox</sup> -O <sub>3</sub> Si(CH <sub>2</sub> ) <sub>11</sub> S(CH <sub>2</sub> ) <sub>2</sub> SO <sub>3</sub> H	5.8 ± 0.9	5.9 ± 1.7
PDMS <sup>ox</sup> -O <sub>3</sub> Si(CH <sub>2</sub> ) <sub>11</sub> S(CH <sub>2</sub> ) <sub>2</sub> (OCH <sub>2</sub> CH <sub>2</sub> ) <sub>4</sub> OH	5.6 ± 1.3	5.0 ± 1.7
PDMS <sup>ox</sup> -O <sub>3</sub> Si(CH <sub>2</sub> ) <sub>2</sub> CF(CF <sub>3</sub> )CF <sub>2</sub> CF(CF <sub>3</sub> ) <sub>2</sub>	3.4 ± 1.2	3.8 ± 1.6
PDMS <sup>ox</sup> -O <sub>3</sub> Si(CH <sub>2</sub> ) <sub>15</sub> CH <sub>3</sub>	3.4 ± 1.4	3.8 ± 1.7
Silastic pump grade tubing	2.3 ± 1.5	2.4 ± 1.4
Polyethylene	1.7 ± 0.8	2.2 ± 1.4

with -COOH and -SO<sub>3</sub>H both had the highest levels of fibrinogen deposition, followed by the -(CH<sub>2</sub>CH<sub>2</sub>O)<sub>4</sub>H, -CF<sub>3</sub>, and -CH<sub>3</sub> surfaces while RX Pump Grade tubing and PE had the lowest levels of deposition. The fibrinogen/fibrin profiles closely parallel the platelet deposition profiles for all of the materials tested. The similarity in the trends of the platelet and fibrinogen/fibrin deposition profiles indicates fibrinogen incorporation into the thrombi, possibly by binding to specific receptor sites on activated platelets, or by incorporation into the thrombi as fibrin strands linking the platelets together [37].

Statistical evaluation of the thrombogenicity of the materials was performed by ranking each material at each time point from the highest to the lowest level of platelet deposition. This was repeated for the fibrinogen/fibrin deposition data. A relative rank was assigned

(highest = 7 and lowest = 1) to each material at each blood-contacting time, and the relative ranks at all blood contacting times were averaged for each material. Table 3 summarizes the platelet and fibrinogen ranks for the materials tested. Table 3 shows similar trends as Figs. 1 and 2, namely that the -COOH, -SO<sub>3</sub>H and -(CH<sub>2</sub>CH<sub>2</sub>O)<sub>4</sub>H surfaces were the most thrombogenic. The -CF<sub>3</sub> and -CH<sub>3</sub> surfaces showed intermediate behavior and RX Pump grade tubing and PE had the lowest levels of platelet and fibrinogen deposition. The reason that the -(CH<sub>2</sub>CH<sub>2</sub>O)<sub>4</sub>H surface appears more thrombogenic in Table 3 is due to its high thrombogenicity at early time points. Of greater importance, however, is the maximum in platelet deposition observed between 20 and 30 min, so that the -(CH<sub>2</sub>CH<sub>2</sub>O)<sub>4</sub>H surface can be considered to have intermediate thrombogenicity.

Analysis of these surfaces using scanning electron microscopy at 5 min of blood exposure (data not shown) showed all surfaces to be covered with a submonolayer of pseudopodial platelets, although the  $-(\text{CH}_2\text{CH}_2\text{O})_4\text{H}$  and  $-\text{SO}_3\text{H}$  surfaces showed very small ( $5\ \mu\text{m}$ ) platelet aggregates. The control RX Pump grade tubing surfaces remained largely the same after 15 min (Fig. 3). At this time point, PE,  $-(\text{CH}_2\text{CH}_2\text{O})_4\text{H}$ , and  $-\text{CH}_3$  showed a few small ( $10\ \mu\text{m}$ ) platelet aggregates, and  $-\text{CF}_3$  showed slightly larger ( $30\ \mu\text{m}$ ) platelet aggregates. Among the more thrombogenic materials,  $-\text{COOH}$  showed  $50\ \mu\text{m}$  platelet aggregates and adherent leukocytes. The  $-\text{SO}_3\text{H}$  surface showed fibrin and entrapped erythrocytes at 15 min of blood contact.

At 30 min of blood-contacting time (Fig. 4), at or just subsequent to the thromboembolytic peak, PE showed platelet aggregates up to  $50\ \mu\text{m}$  in size, with occasional adherent leukocytes and fibrin. RX Pump grade tubing

and the  $-\text{CH}_3$ , and  $-\text{CF}_3$  surfaces showed similar-sized thrombi, with occasional leukocytes, erythrocytes, and fibrin. The  $-(\text{CH}_2\text{CH}_2\text{O})_4\text{H}$  surfaces showed similar behavior to PE and RX Pump grade tubing, with  $50\ \mu\text{m}$  platelet thrombi, and areas of adherent, spread leukocytes, as well as areas of fibrin meshwork. The  $-\text{COOH}$  and  $-\text{SO}_3\text{H}$  surfaces showed very large ( $>100\ \mu\text{m}$ ) complex mural thrombi, consisting of platelets, leukocytes, fibrin, and entrapped erythrocytes.

After 1 h of exposure to blood, PE showed similar behavior as at 30 min, with  $50\ \mu\text{m}$  platelet thrombi, but larger numbers of adherent, spread leukocytes. RX Pump grade tubing showed only platelets and adherent leukocytes, but no thrombi. The  $-\text{CH}_3$  and  $-\text{CF}_3$  surfaces were quite similar to PE control, with  $50\ \mu\text{m}$  platelet thrombi, and adherent, spread leukocytes. The  $-(\text{CH}_2\text{CH}_2\text{O})_4\text{H}$  surface showed monolayers of adherent, spread leukocytes. The  $-\text{COOH}$  and  $-\text{SO}_3\text{H}$  surfaces

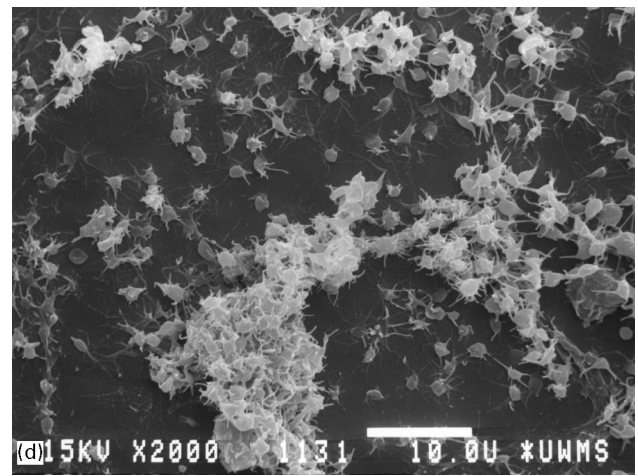
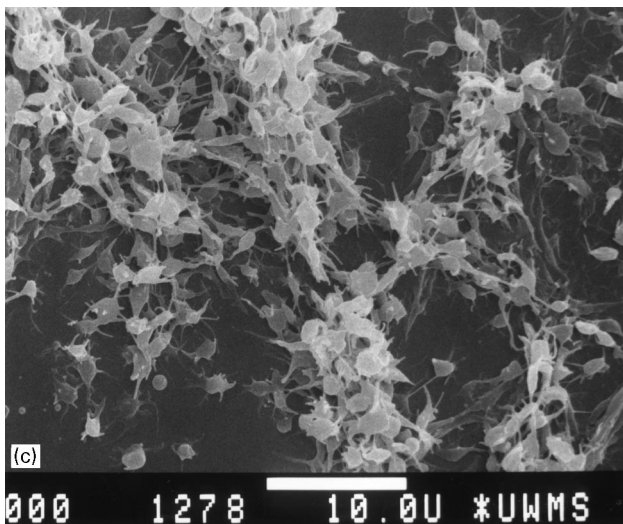
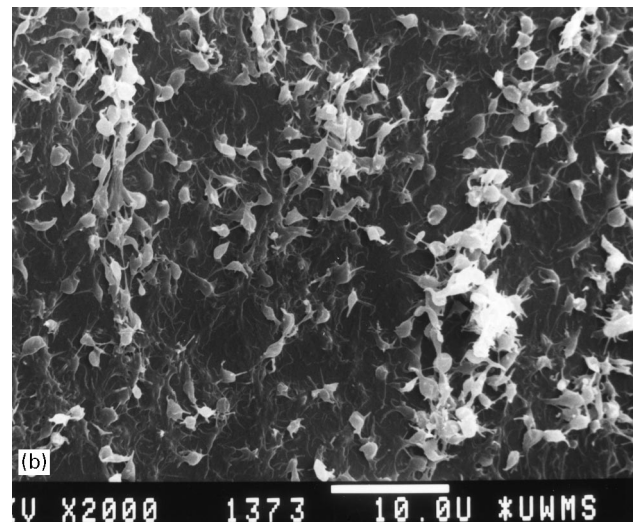
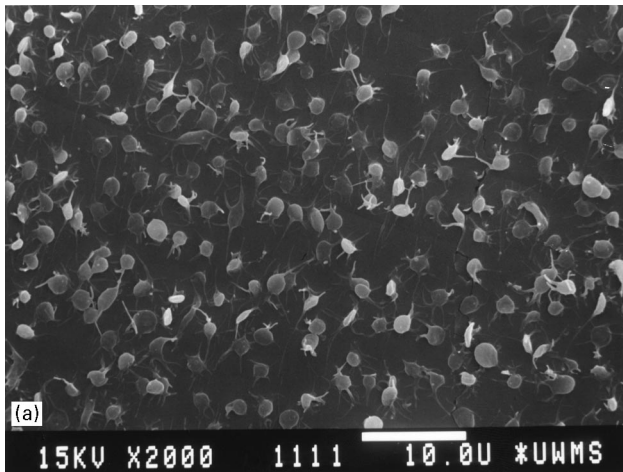


Fig. 3. Scanning electron micrographs for test surfaces after 15 min of blood exposure. (a) RX; (b) PE; (c)  $\text{CH}_3$ ; (d)  $\text{CF}_3$ ; (e)  $(\text{EO})_4$ ; (f)  $\text{CO}_2\text{H}$  and (g)  $\text{SO}_3\text{H}$ . (Scale bar equals  $10\ \mu\text{m}$ .)

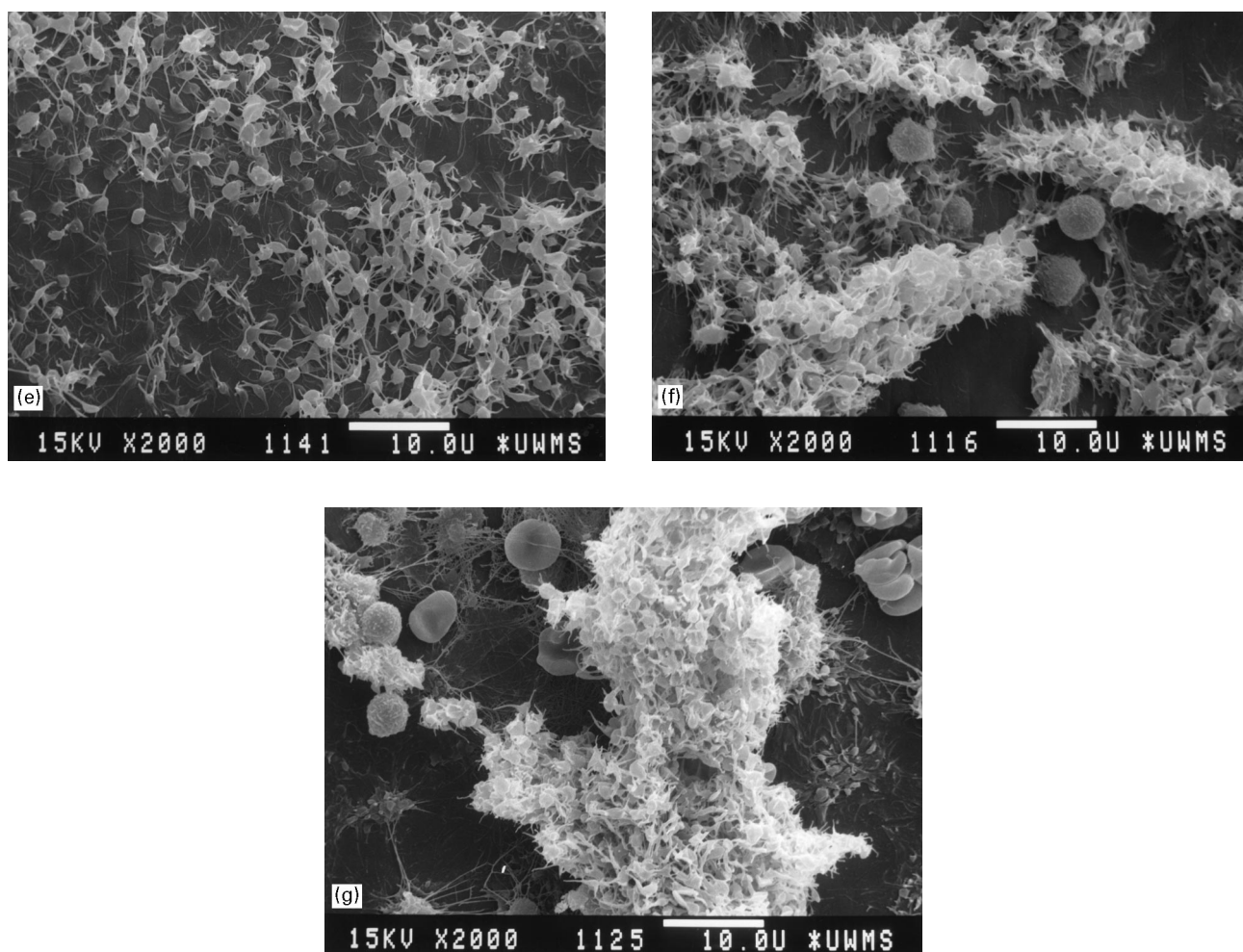


Fig. 3. (continued).

remained the most thrombogenic at 60 min, as at 30 min, and showed complex mural thrombi ( $> 100 \mu\text{m}$ ), consisting of platelets, leukocytes, fibrin, and entrapped erythrocytes.

The  $-(\text{CH}_2\text{CH}_2\text{O})_4\text{H}$  monolayer showed comparable behavior to a monolayer studied earlier which contained a shorter ethylene oxide end group,  $-(\text{CH}_2\text{CH}_2\text{O})_3\text{H}$  [14]. It appears that a difference in one ethylene oxide group does not affect the thrombogenicity of the material. Both these surfaces had an intermediate thrombogenicity. No comparisons can be done with work performed on thiol self-assembled monolayers since this work was performed *in vitro* [20, 21].

Platelet and fibrinogen adhesion seem to increase on the  $\text{PDMS}^{\text{ox}}-\text{O}_3\text{Si}(\text{CH}_2)_{15}\text{CH}_3$  surface with respect to the shorter alkyl chain  $\text{PDMS}^{\text{ox}}-\text{O}_3\text{Si}(\text{CH}_2)_9\text{CH}_3$  studied earlier. This can be an indication that surface mobility (higher in the case of the shorter alkyl chain) can lead to better biocompatibility. Indeed, the biocompatible properties of ethylene oxide containing polymers have been attributed by some researchers to the high mobility of the chains [38].

Evaluation of the hemocompatibility of these materials using a canine *ex vivo* series shunt model showed that the sulfonated and carboxylated monolayers are extremely thrombogenic, in contrast to previous work with sulfonated polyurethanes. This result is consistent with the observation that under certain conditions, heparin can cause platelet activation [39]. Further, Lai et al. [40] studied the response of column-washed platelets to sulfonated polyurethanes *in vitro* under static conditions, and found that platelet membranes become disrupted, although protein-surface interactions may modulate this response *in vivo*. Takahara et al. synthesized a series of polyurethaneureas which contained long, hydrophilic side chains in the soft segment [41]. Sulfonate groups were incorporated at the end of the side chains. At the lowest levels of sulfonate incorporation, there was a slight improvement in blood compatibility, but at higher levels of sulfonation, the materials were actually more thrombogenic than controls. Further, chromic acid-oxidized polyethylene, which contains numerous carboxylate groups on the surface, has been observed to be

extremely thrombogenic [31]. It may be that the surface density of the sulfonate groups is too high in the present case, so that it may be possible to reduce the level of platelet deposition by reducing the density of sulfonate groups. Further, since the sulfonated polyurethanes are a phase-separated material, it may be that the spatial distribution of sulfonate groups is important. This issue could be addressed using microfabrication techniques to control the spatial resolution of the self-assembled monolayer [42].

#### 4. Conclusions

Evaluation of the hemocompatibility of the surface modified silastic tubing using a canine ex vivo series

shunt experiment showed that PDMS<sup>ox</sup>-O<sub>3</sub>Si(CH<sub>2</sub>)<sub>11</sub>-S(CH<sub>2</sub>)<sub>2</sub>SO<sub>3</sub>H, and PDMS<sup>ox</sup>-O<sub>3</sub>Si(CH<sub>2</sub>)<sub>10</sub>COOH are the most thrombogenic surfaces. In contrast, polyethylene and PDMS silastic tubing which were used as controls were found to have the lowest fibrinogen and platelet deposition at all times. PDMS<sup>ox</sup>-O<sub>3</sub>Si(CH<sub>2</sub>)<sub>15</sub>CH<sub>3</sub>, PDMS<sup>ox</sup>-O<sub>3</sub>Si(CH<sub>2</sub>)<sub>2</sub>CF(CF<sub>3</sub>)CF<sub>2</sub>CF(CF<sub>3</sub>)<sub>2</sub> and PDMS<sup>ox</sup>-O<sub>3</sub>Si(CH<sub>2</sub>)<sub>11</sub>S(CH<sub>2</sub>)<sub>2</sub>(OCH<sub>2</sub>CH<sub>2</sub>)<sub>4</sub>OH were found to exhibit an intermediate thrombogenicity.

The presence of the ethylene oxide functionality did not result in a significantly more thromboresistant surface. However, the ethylene oxide chain lengths used in the current study were much shorter than those used by other investigators and may also have been too densely packed to have the high mobility which is hypothesized to reduce protein adsorption [16, 43]. Increasing the

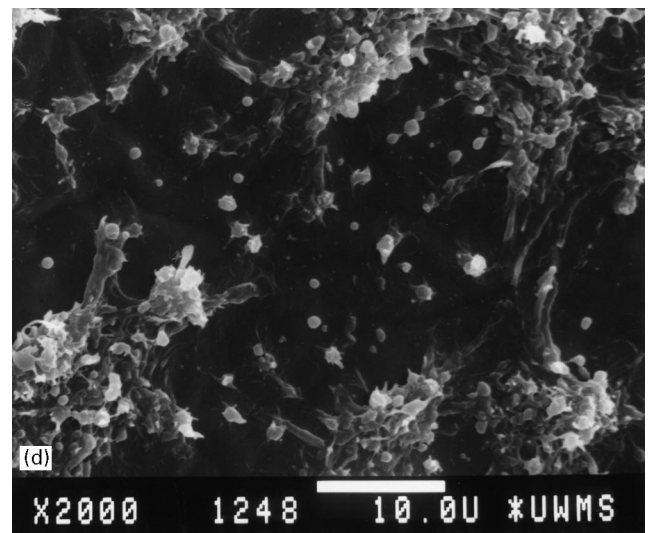
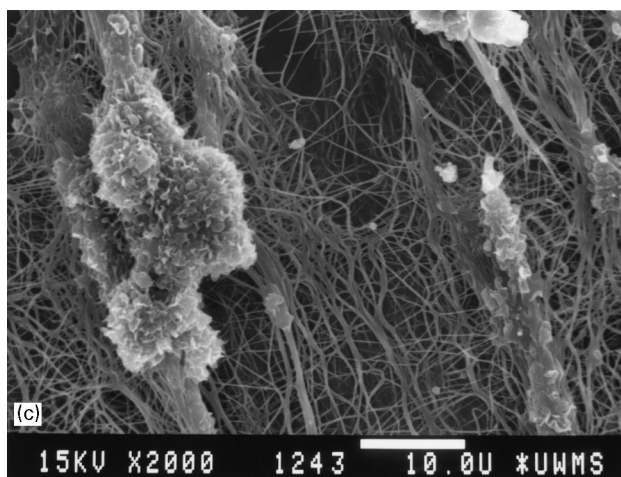
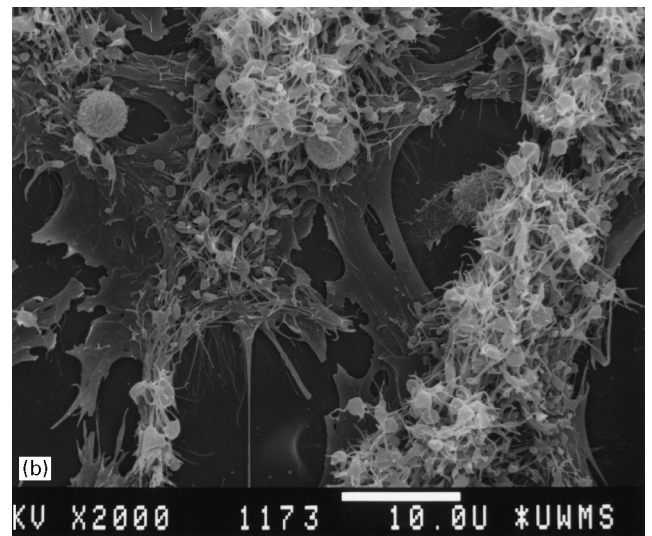
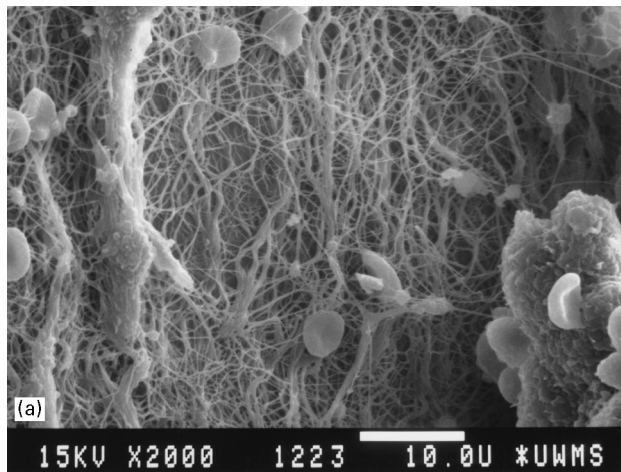


Fig. 4. Scanning electron micrographs for test surfaces after 30 min of blood exposure. (a) RX; (b) PE; (c) CH<sub>3</sub>; (d) CF<sub>3</sub>; (e) (EO)<sub>4</sub>; (f) CO<sub>2</sub>H and (g) SO<sub>3</sub>H. (Scale bar equals 10 μm.)

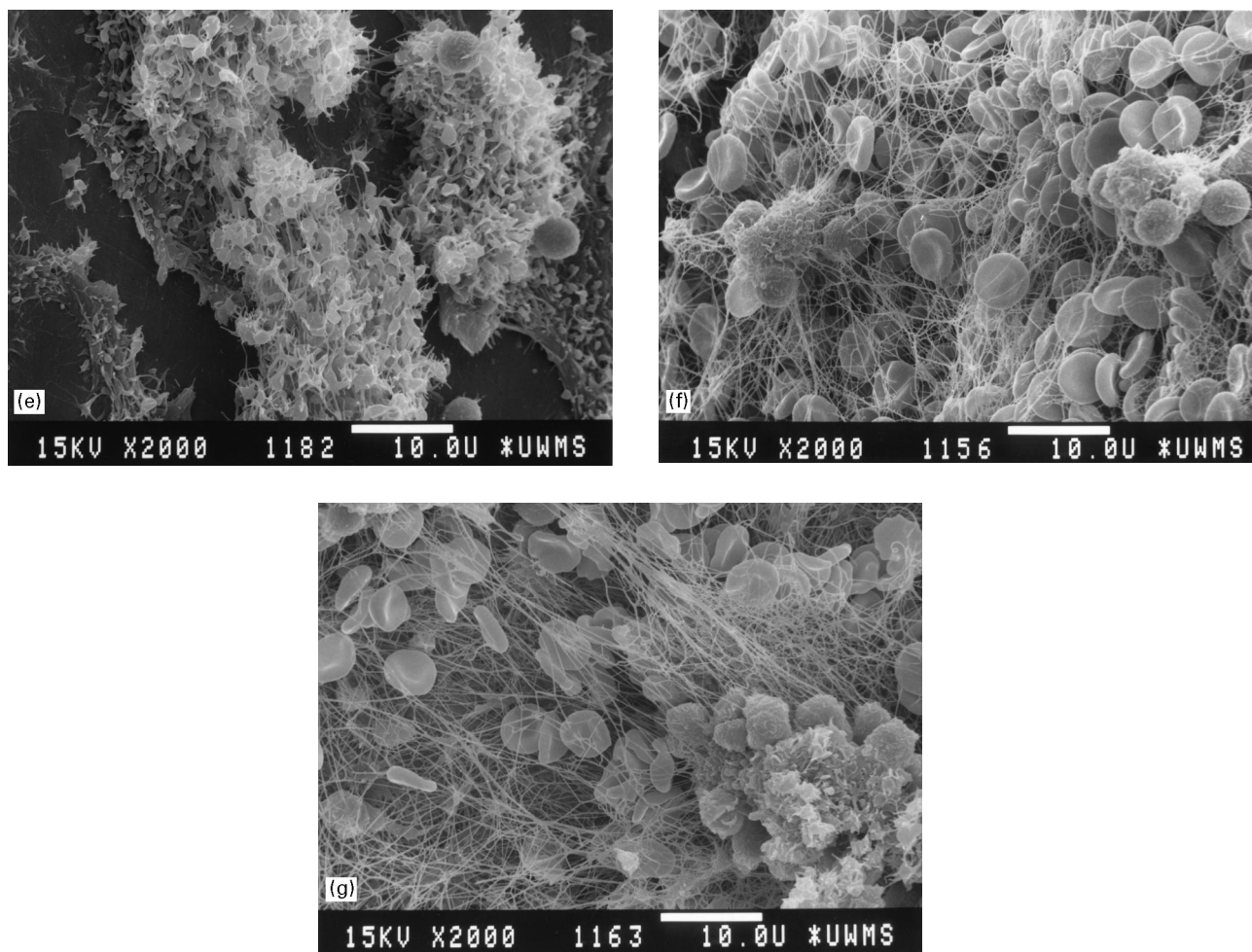


Fig. 4. (continued).

ethylene oxide chain length by a single group did not affect the blood compatibility of these surfaces.

The  $-\text{CH}_3$  surface evaluated in this study, with an alkyl chain length of 15 methylene units, was considerably more thrombogenic than a similar material with a shorter alkyl tail (9 methylene units) evaluated previously [14]. While the present material showed a thromboembolytic peak of approximately 2000 platelets per  $1000 \mu\text{m}^2$ , the latter showed a maximum platelet deposition of only 300 platelets per  $1000 \mu\text{m}^2$ . Assuming that a greater degree of crystallinity has been introduced in the present series, this would suggest that the more mobile, liquid-like surface created by the smaller alkyltrichlorosilane, is more thromboresistant. The fluorinated surfaces showed the best behavior among the surface modified elastomers. The control surfaces, PE and silicone rubber, were less thrombogenic than in the previous work, so that animal-to-animal variation cannot account for some of the differences between the crystalline and liquid-like monolayers.

### Acknowledgements

Technical assistance was provided by Larry Whitesell (animal surgery), Everett Clover (scanning electron spectroscopy), and Arlene P. Hart (hematology). This work was supported in part by the National Institutes of Health, through grants HL-24046 and HL-47179, and the Dow Corning Corp., Midland, MI.

### References

- [1] Tyler BJ, Ratner BD, Castner DG, Briggs D. Variations between Biomer lots. I. Significant differences in the surface chemistry of two lots of a commercial poly(etherurethane). *J Biomed Mater Res* 1992;26:273–89.
- [2] Silver JH, Lewis KB, Ratner BD, Cooper SL. The effect of polyol type on the surface structure of sulfonate-containing polyurethanes. *J Biomed Mater Res* 1993;27:735–45.
- [3] Dulsey CS, Georger JHJ, Krauthamer V, Stenger DA, Fare TL, Calvert JM. Deep UV photochemistry of chemisorbed

- monolayers: patterned coplanar molecular assemblies. *Science* 1991;252:551–4.
- [4] Bain CD, Whitesides GM. Molecular-level control over surface order in self-assembled monolayer films of thiols on gold. *Science* 1988;240:62–3.
- [5] Stenger DA, Georger JH, Dulcey CS, Hickman JJ, Rudolph AS, Nielsen TB, McCort SM, Calvert JM. Coplanar molecular assemblies of amino- and perfluorinated alkylsilanes: characterization and geometric definition of mammalian cell adhesion and growth. *J Am Chem Soc* 1992;114:8435–42.
- [6] Chaudhury MK, Whitesides GM. Direct measurement of interfacial interactions between semispherical lenses and flat sheets of poly(dimethylsiloxane) and their chemical derivatives. *Langmuir* 1991;7:1343–63.
- [7] Chaudhury MK, Whitesides GM. Correlation between surface free energy and surface constitution. *Science* 1992;255:1230–2.
- [8] Chaudhury MK, Owen MJ. Correlation between adhesion hysteresis and phase state of monolayer films. *Phys Chem* 1993;97:5722–6.
- [9] Ferguson GS, Chaudhury MK, Biebuyck HA, Whitesides GM. Monolayers on disordered substrates: self-assembly of alkyltrichlorosilanes on surface-modified polyethylene and poly(dimethylsiloxane). *Macromolecules* 1993;26:5870–5.
- [10] Collinson M, Bowden E, Tarlov MJ. Voltametry of covalently immobilized cytochrome c on self-assembled monolayer electrodes. *Langmuir* 1992;8:1247–50.
- [11] Lewandowska K, Pergament E, Sukenik CN, Culp LA. Cell-type-specific adhesion mechanisms mediated by fibronectin adsorbed to chemically derivatized substrata. *J Biomed Mater Res* 1992;26:1343–63.
- [12] Margel S, Vogler EA, Firment L, Watt T, Haynie S, Sogah DY. Peptide, protein, and cellular interactions with self-assembled monolayer model surfaces. *J Biomed Mater Res* 1993;27:1463–76.
- [13] Chaudhury MK. Surface free energies of alkylsiloxane monolayers supported on elastomeric polydimethylsiloxanes. *J Adhes Sci Technol* 1993;7:669–75.
- [14] Silver JH, Hergenrother RW, Lin J-C, Lim F, Lin H-B, Okada T, Chaudhury MK, Cooper SL. Surface and blood-contacting properties of alkylsiloxane monolayers supported on silicone rubber. *J Biomed Mater Res* 1995;29:535–48.
- [15] Bonhert JL, Fowler BC, Horbett TA, Hoffman AS. Plasma gas discharge deposited fluorocarbon polymers exhibited reduced elutability of adsorbed albumin and fibrinogen. *Biomater Sci Polym Edn* 1990;1:279.
- [16] Kiaei D, Hoffman AS, Ratner BD, Horbett TA. Interaction of blood with gas discharge treated vascular grafts. *J Appl Poly Sci: Appl Polym Symp* 1988;42:269–83.
- [17] Yu X-H, Okkema AZ, Cooper SL. Synthesis and physical properties of poly(fluoroalkylether)-urethanes. *J Appl Polym Sci* 1990;1:1777–95.
- [18] Brinkman E, Poot A, van der Does L, Bantjes A. Platelet deposition studies on copolyether-urethanes modified with poly(ethylene oxide). *Biomaterials* 1990;11:200–5.
- [19] Chaikof EL, Merrill EW, Callow AD, Connolly RJ, Verdon SL, Ramberg K. PEO enhancement of platelet deposition, fibrinogen deposition and complement C3 activation. *J Biomed Mater Res* 1992;26:1163–8.
- [20] Prime KL, Whitesides GM. Self-assembled organic monolayers: model systems for studying adsorption of proteins at surfaces. *Science* 1991;252:1164–7.
- [21] Ista LK, Fan H, Baca O, Lopez GP. Attachment of bacteria to model solid surfaces: oligo(ethylene glycol) surfaces inhibit bacterial attachment. *FEMS Microbiol Lett* 1996;142:59–63.
- [22] Casu B. Structure of heparin and heparin fragments. *Ann NY Acad Sci* 1989;556:1–17.
- [23] Jozefowitz M, Jozefonvicz J. Antithrombogenic polymers. *Pure Appl Chem* 1984;56:1335–44.
- [24] Mauzac M, Aubert N, Jozefonvicz J. Antithrombic activity of some polysaccharide resins. *Biomaterials* 1982;3:221–4.
- [25] Ito Y, Iguchi Y, Kashiwagi T, Imanishi Y. Synthesis and non-thrombogenicity of polyetherurethaneurea film grafted with poly(sodium vinyl sulfonate). *J Biomed Mater Res* 1991;25:1347–61.
- [26] Okkema AZ, Visser SA, Cooper SL. Physical and blood-contacting properties of polyurethanes based on a sulfonic acid-containing diol chain extender. *J Biomed Mater Res* 1991;25:1371–95.
- [27] Silver JH, Hart AP, Williams EC, Cooper SL, Charef S, Labarre D, Jozefowitz M. Anticoagulant effects of sulfonated polyurethanes. *Biomaterials* 1992;13:339–43.
- [28] Okkema AZ, Yu X-H, Cooper SL. The physical and blood-contacting properties of propyl sulfonate grafted Biomer<sup>®</sup>. *Biomaterials* 1991;12:3–12.
- [29] Han DK, Jeong SY, Kim YH, Min BG, Cho HI. Negative cilia concept for thromboresistance: synergistic effect of PEO and sulfonate groups grafted onto polyurethanes. *J Biomed Mater Sci* 1991;25:561–75.
- [30] Santerre JP, ten Hove P, VanderKamp NH, Brash JN. Effect of sulfonation of segmented polyurethanes on the transient adsorption of fibrinogen from plasma. Possible correlation with anticoagulant behavior. *J Biomed Mater Sci* 1992;26:39–57.
- [31] Lelah MD, Lambrecht LK, Cooper SL. A canine ex vivo series shunt for evaluating thrombus deposition on polymer surfaces. *J Biomed Mater Sci* 1984;18:475–96.
- [32] Wasserman SR. PhD Thesis. Harvard University, 1989.
- [33] Lelah D, Grasel TG, Pierce JA, Cooper SL. The measurement of contact angles on circular tubing surfaces using the captive bubble technique. *J Biomed Mater Sci* 1985;19:1011–5.
- [34] Park KD, Mosher DF, Cooper SL. Acute surface-induced thrombosis in the canine ex vivo model: importance of protein composition of the initial monolayer and platelet activation. *J Biomed Mater Res* 1986;20:589–612.
- [35] Zanker A. Detection of outliers by means of Nalimov's test. *Chem Eng* 1984;91:74.
- [36] Takahara A, Okkema AZ, Cooper SL, Coury SJ. Effect of surface hydrophilicity on ex vivo blood compatibility of segmented polyurethanes. *Biomaterials* 1991;12:324–34.
- [37] Grasel TG, Cooper SL. Surface properties and blood compatibility of polyurethaneureas. *Biomaterials* 1986;7:315–28.
- [38] Park KD, Okano T, Nojiri C, Kim SW. Heparin immobilization on segmented polyurethaneurea surfaces—effect of hydrophilic spacers. *J Biomed Mater Sci* 1988;22:977–92.
- [39] Brace LD, Fareed J. An objective assessment of the interaction of heparin and its fractions with human platelets. *Sem Thromb Hemost* 1985;11:190–8.
- [40] Lai QJ, Albrecht RM, Cooper SL. Effects of polyurethane surface chemistry on fibrinogen receptor expression on adhered platelets under static and flow conditions. In: AIChE, 2nd Topical Conf on Emerging Technologies in Materials. San Francisco, CA, 1989.
- [41] Takahara A, Okkema AZ, Wabers H, Cooper SL. Effect of hydrophilic soft segment side chains on the surface properties and blood compatibility of segmented poly(urethaneureas). *J Biomed Mater Res* 1991;25:1095–118.
- [42] Bhatia SK, Teixeira JL, Anderson M, Shriver-Lake LC, Calvert JM, Georger J, Hickman JJ, Dulcey CS, Schoen PE, Ligler FS. Fabrication of surfaces resistant to protein adsorption and application to two dimensional protein patterning. *Anal Biochem* 1993;208:197–205.
- [43] Desai NP, Hubbell JA. Biological responses to polyethylene oxide modified polyethylene terephthalate surfaces. *J Biomed Mater Res* 1991;25:829–43.